

Removal of heavy metals by homolytically functionalized poly(acrylic acid) with hydroquinone

Saâd Moulay¹ · Nabila Bensacia¹

Received: 25 June 2015 / Accepted: 28 August 2016 / Published online: 12 September 2016
© The Author(s) 2016. This article is published with open access at Springerlink.com

Abstract Poly(acrylic acid) (PAA) was synthesized and chemically modified with hydroquinone (HQ) applying the reaction conditions of Minisci. A degree of modification of as high as 32 % was obtained under optimal conditions: temperature of 70–80 °C, time of 5 h, and [*p*-benzoquinone]/[acrylic acid] ratio of 1.25. The synthesized PAA and its modified form HQ-PAA were characterized by UV–visible, FT-IR, XRD, SEM, ¹³C NMR spectroscopy, TGA, DSC, and size exclusion chromatography. The study of copper (II) adsorption by the cross-linked PAA and HQ-PAA resins was undertaken, varying the following parameters: pH, time, temperature, ionic strength, sorbent mass, and initial copper (II) concentration. Optimal copper sorption extents of 5.5 and 20 mg g⁻¹ for PAA and HQ-PAA resins, respectively, were found under the following conditions: a pH of 5.4, a time of 3 h, a temperature of 45 °C, and an ionic strength of 0. Sorbent resins were achieved by cross-linking poly(acrylic acid) and its modified one through an oxidative decarboxylation process.

Keywords Copper · Hydroquinone · Metallic adsorption · Poly(acrylic acid)

Introduction

Polyacrylics are a special class of polymers as far as their uses, and applications are of interest. Their nowadays ubiquity stems from the large spectrum of their properties which are on a par with the chemical reactivity of their functional groups, i.e., carboxylic, ester, amide, and nitrile. A wide range of their chemical modifications are, but the result of the proneness of these groups to chemical reactions, affording valuable materials with targeted properties. Poly(acrylic acid) (PAA), coined the name “*carbopol*” in pharmaceuticals, is known to be a super absorbent polymer that can absorb and retains a great extent of water, a property that is exploited in hydrogels making for various controlled drug delivery systems [1, 2]; a related fact is that the swelling behavior of PAA hydrogels was found to be highly medium pH dependent due to the presence of carboxylic groups [3]. Low molecular weight PAA has been valorized as an efficient salt-scaling inhibitor, chiefly in oilfield operations, via the ability of the carboxylic groups in sequestering metal ions [4]. A five-fold enhancement in the removal heavy metals was observed with PAA-bound tetrahydroxybenzene (THB-PAA) with respect to the virgin PAA [5]. Pyridylazo-2-naphthol-functionalized PAA was employed as a fluorescent nanofiber probe for the determination of Ni²⁺ [6]. Besides of being water soluble, PAA has a capacity to form polyelectrolyte complex nanoparticles with other polymers, such as poly(ethyleneimine) [7]. Ultrathin films for electrochromic devices were made via a layer-by-layer (LBL) strategy by reacting PAA with polyaniline in acid–base (COOH/NH₂) mechanism [8]. By the virtue of its carboxylic groups, PAA served as template for making helical polyaniline-PAA microwires or rods [9]. The plausible decarboxylation of PAA via a homolytic pathway promoted its use as a redox

✉ Saâd Moulay
polymchemlab@hotmail.com; saadmoulay@univ-blida.dz

¹ Laboratoire de Chimie-Physique Moléculaire et Macromoléculaire, Département de Chimie Industrielle, Faculté de Technologie, Université Saâd Dahlab de Blida, B. P. 270, Route de Soumâa, 09000 Blida, Algeria

unit carrier [10]. Apart from its hydrophilic character, PAA via its carboxylic groups was of a critical value in coating bleomycin-loaded magnetite nanoparticles (Fe_3O_4) to generate an antitumoral drug delivery system [11]. As for polycarboxylic acids [12], the other facet of PAA is its propensity towards potentiometric titration. The latter property is of a great merit, because the pH plays a pivotal role in several investigations, indicating the actual form of the involved molecule (ionized and neutral species). Moreover, the polymer effect emerges in various chemical studies as the results using polymers may be different from those using their molecular counterparts; for example, the potentiometric titration of PAA exhibits a profile different from those of acrylic acid and acetic acid.

In a continuation of a previous work [5, 13, 14], it is herein intended in the present paper to apply the chemistry of Minisci [15] at the macromolecular level, and henceforth to the chemical modification of poly(acrylic acid) (PAA) with hydroquinone (**HQ**); the latter one, being a polyhydroxylated benzene, is conceived as ligating species in the removal of heavy metallic ions via adsorption process. A synergism of COOH and **HQ** functionalities within the polymeric material in the removal of heavy metals is herein demonstrated; introducing **HQ** moieties onto PAA matrix would enhance the metal adsorption capacity of this polymer. Recently, we reported the results of adsorption of cadmium and led by COOH-functionalized mesoporous silica [16, 17]. Resins containing catechol and resorcinol were evaluated as sorbents for heavy metal ions [18, 19]. The present study includes the preparation of the **HQ**-PAA resin and an observation of the effects of reaction time and benzoquinone/monomer unit molar ratio on the degree of substitution, and of the effects of several experimental parameters, such as contact time, initial pH, electrolyte concentration, temperature, and initial resin mass, and copper concentration on the capacity exchange in the metal adsorption. The adsorption kinetics and isotherm models were used to describe the copper adsorption data. The thermodynamic factors of adsorption were determined.

Experiment

Materials and measurements

The chemicals were purchased from one of the following chemical companies: Aldrich (France), Fluka AG, Prolabo, and Merck. Acrylic acid was purified by vacuum distillation. Azobisisobutyronitrile (AIBN) was recrystallized from methanol. 1,4-Benzoquinone (BQ) was used as purchased. UV-vis spectra were recorded using a JASCO UV-

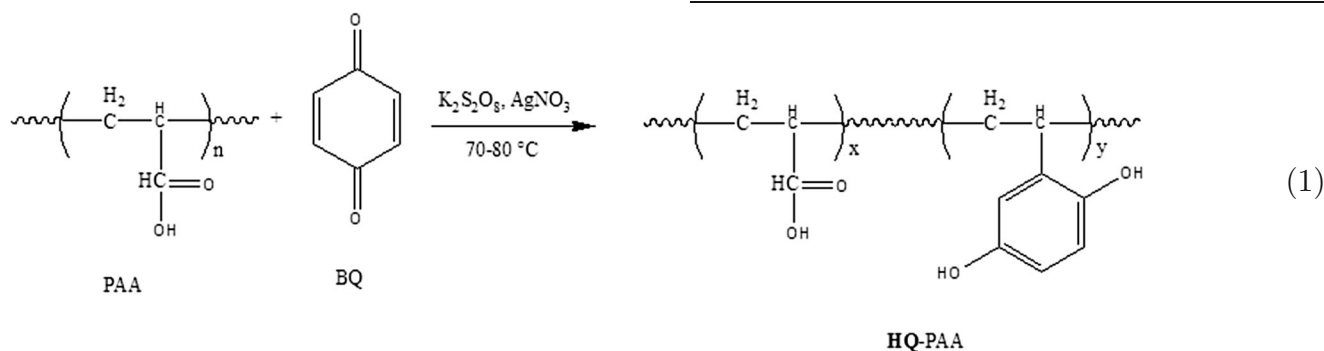
Vis spectrophotometer using bidistilled water as a solvent. Infrared spectra were taken with a JASCO 4200 FT-IR. The polymer samples for the infrared analysis were in the form of cast films. The diagrams of X-ray diffraction (XRD) were recorded on a Bruker D8 diffractometer (K radiation, $\lambda = 0.154$ nm, 40 kV, 100 mA). The experiments were performed directly on the polymer samples which were finely cut in the range of 2θ equal to 5° – 90° at the scanning speed of $0.02^\circ/\text{s}$. The morphology of polymeric samples was observed using a scanning electron microscope (SEM) JEOL 6700 operating at an acceleration voltage of 200 kV. ^{13}C NMR spectra were recorded using a spectrometer Bruker 400 MHz using CD_3OD as the solvent. Molecular weights were measured by size exclusion chromatography (SEC) [gel permeation chromatography (GPC)] on a set DIONEX, series Ultimate 3000 (degasser, pump, autosampler), 4 Shodex OH-pack 30 cm in series (803HQ, 804HQ, 806HQ, and 807HQ), a differential refractometer OPTILABrEX (Wyatt Tech), and a light-scattering detector DAWN multiangle HELEOSII (Wyatt Tech). The eluent was an aqueous solution consisting of water and 0.1 M NaNO_3 at a rate of 0.5 mL min^{-1} . The injected volume was 0.1 mL from a concentration of 2 – 3 g mL^{-1} of each polymer solution. Differential scanning calorimetry (DSC) thermograms were recorded on Netzsch DSC 204 F1 at a heating rate of 5 $^\circ\text{C}$ min^{-1} under nitrogen atmosphere. Thermogravimetric analysis (TGA) was conducted on NETZSCH TG 209 F3 apparatus in the temperature interval of 20 – 600 $^\circ\text{C}$, at a heating rate of 10 $^\circ\text{C}$ min^{-1} under nitrogen atmosphere (2 mL min^{-1}). The used weights of polymer samples for the measurement were in the range of 5.5 – 5.7 mg. Metallic adsorption by resins was estimated by flame atomic absorption spectrometer (FAAS) of type Buck Scientifics 210VGP fitted with a deuterium lamp, a corresponding hollow cathode lamp, and a 10-cm long burner; the flame was provided by air-acetylene gas.

Modification reactions of poly(acrylic acid) PAA (Eq. 1)

In a 500 mL, one-neck round bottom flask equipped with a condenser 0.5 g (6.94×10^{-3} mol) of PAA was dissolved in 50 mL of distilled water, followed by the addition of 50 mL of an ethanolic solution containing 0.93 g (8.6×10^{-3} mol) of BQ. To this homogeneous mixture, 0.039 g (2.3×10^{-4} mol) of silver nitrate was added, followed by the addition of 150 mL of distilled water. The system was heated to reach 75 – 80 $^\circ\text{C}$ under magnetic stirring. Once this temperature was reached, a saturated solution of potassium persulfate (1.88 g, 6.95×10^{-3} mol)

was added dropwise. The reaction was stopped, and the content was cooled to room temperature. The modified PAA was isolated by the following sequential steps: (1) the evaporation of ethanol followed by the addition of 50 mL of distilled water; (2) the mixture was allowed to stand for 1 day to assure the precipitation of the unreacted BQ (the precipitate was eliminated by filtration); and (3) the modified PAA was obtained by casting from the solution within 4 days. The cast film was then dried to constant weight in vacuo at 45 °C for 4 days.

The modified PAA is herein abbreviated as **HQ-PAA**.



The degree of substitution S (%) was provided by the following equations (Eqs. 2, 3) [10, 20]:

$$S\% = \frac{n_2}{n_1 + n_2} \quad (2)$$

$$n_1 = \frac{m - n_2 M_2}{M_1} \quad (3)$$

where n_2 is the number of moles of **HQ** (in the form of vinyl hydroquinone) present in the modified PAA, estimated from the UV calibration curve of **HQ**; n_1 is the number of moles of acrylic acid present in the **HQ-PAA**,

provided by Eq. (3); m is the sample weight of the **HQ-PAA** used in the UV measurements; M_1 and M_2 are the molecular weights of acrylic acid and vinyl hydroquinone, respectively.

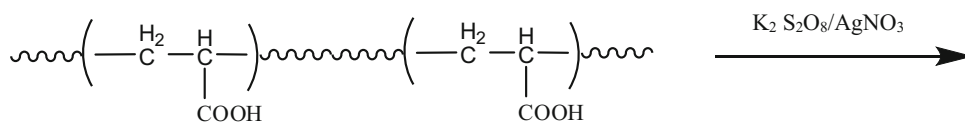
Metallic ion adsorption

Preparation of the resins (Eqs. 4 and 5)

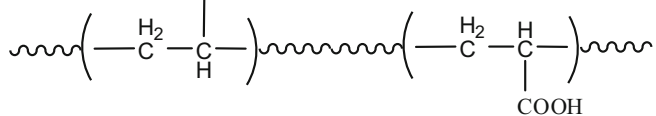
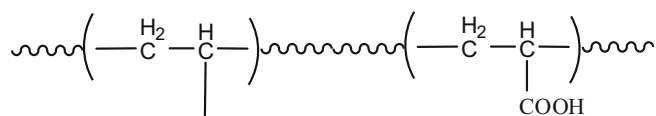
Into a 100 mL round-bottomed flask fitted with a reflux condenser, 5 g of polymer were charged and dissolved in

100 mL of distilled water. An amount of 0.39 g (2.3×10^{-3} mol) of AgNO_3 was added, and the mixture was heated while stirring at a temperature of 70–75 °C, then a 100 mL aqueous solution of 1.88 g (6.96×10^{-3} mol) of $\text{K}_2\text{S}_2\text{O}_8$ was added dropwise to the mixture. The latter was allowed to stir at this temperature domain for almost 1 h, the time after which a precipitate was observed. The precipitate was isolated and washed with a plenty of water and dried to a constant weight in vacuo for 4 days at a temperature of 45 °C.

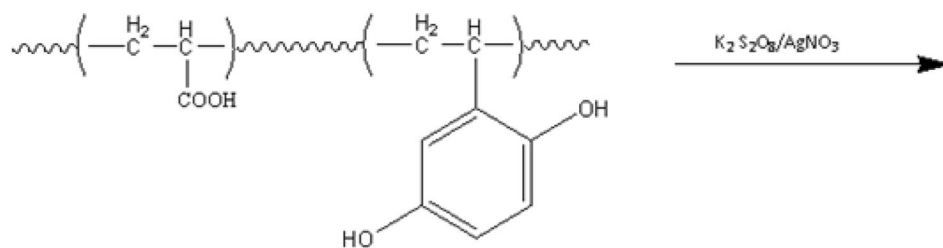




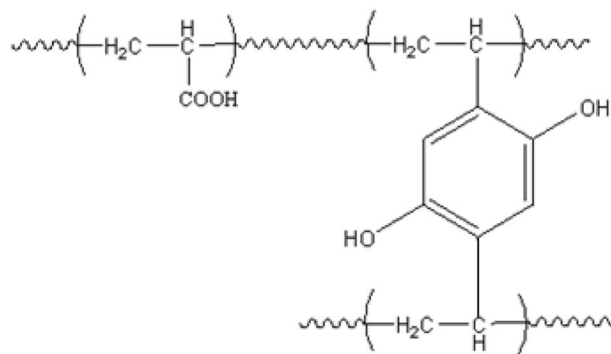
PAA polymer



PAA resin



HQ-PAA



HQ-PAA resin

(5)



Metal ion adsorption/desorption

In a thermostated cell, 0.1 g of cross-linked resin was added to 50 mL of 50 mg L⁻¹ Cu(NO₃)₂ aqueous solution, which was previously adjusted to a desired pH (with 0.1 N HCl and 0.1 N NaOH). The system was stirred with a magnetic bar at a temperature of 30 °C. Sampling of the supernatant liquid was realized at specified time intervals. The adsorption capacity Q_t (in mg of copper per gram of resin) [21] was computed from Eq. 6:

$$Q_t = \frac{(C_0 - C_e) \cdot V}{W} \quad (6)$$

where C_0 , C_e , V , and W are the initial copper concentration in the aqueous solution (mg L⁻¹), the copper concentration at equilibrium (mg L⁻¹), the volume of aqueous solution (L), and the weight of the resin (g), respectively. A triplicate adsorption analysis was undertaken, and the mean values were considered.

The desorption of metal ion from the dried loaded resin (0.2 g) was conducted using 0.1 N HNO₃ (50 mL) at 30 °C for 3 h. The regenerated resin was subjected to two other adsorption–desorption cycles. The desorption percentage DP [22] was calculated according to Eq. 7:

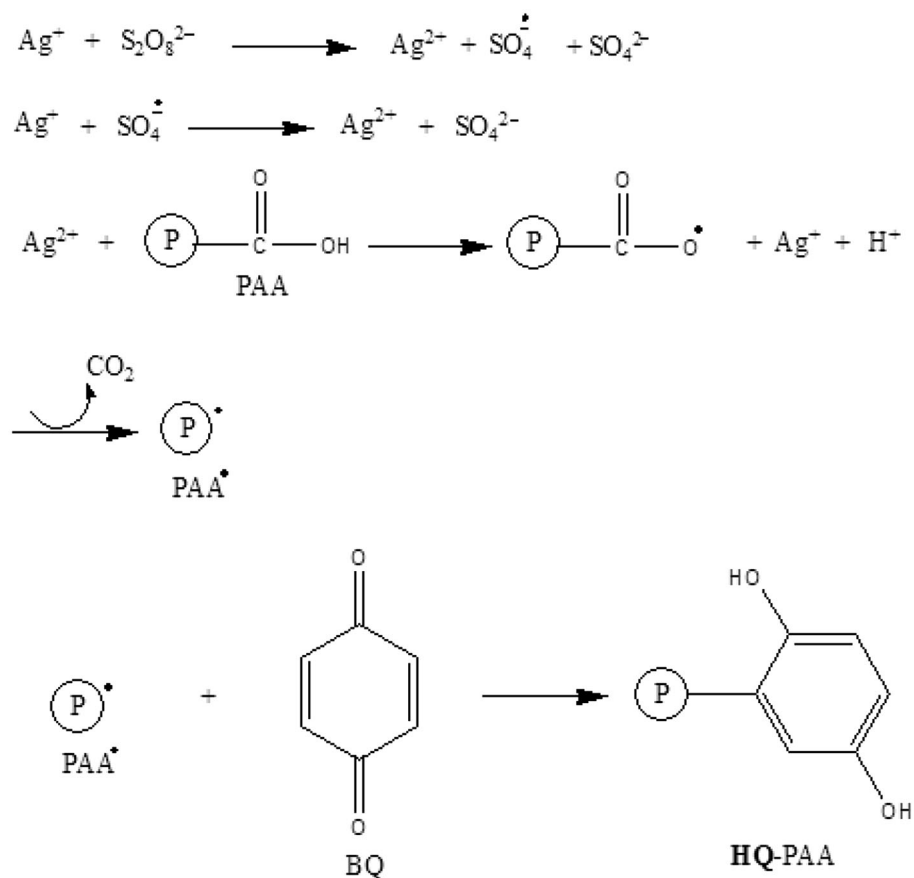
$$DP = \frac{\text{Amount of metallic ion desorbed in the medium}}{\text{Amount of metallic ion present in the resin}} \times 100. \quad (7)$$

Results and discussion

Chemical modification of PAA

Poly(acrylic acid) was synthesized as previously reported [5] and subjected to chemical reaction with *p*-benzoquinone by the virtue of the oxidative decarboxylation conditions of Minisci [13], as traced in Eq. 1. The mechanism proposed for such a chemical modification is depicted in Scheme 1 [23]. The system K₂S₂O₈/AgNO₃ induced the formation of a polymeric radical PAA[•]. Being an electron-rich site and behaving as a nucleophilic alkyl, the latter radical readily reacted with a benzoquinone compound, acting as an electron-deficient species. Minisci advanced such a mechanistic explanation for the homolytic alkylation of pyridine and its derivatives [24, 25]. Nucleophilic alkyl radicals were reported to attack preferentially the carbon atom of the benzoquinone compound [24].

Scheme 1 Mechanism of the grafting of hydroquinone (HQ) on poly(acrylic acid)



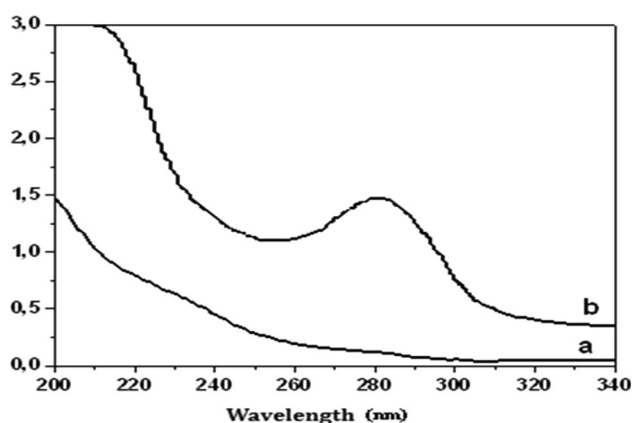


Fig. 1 UV-visible spectra: **a** PAA; **b** HQ-PAA ([BQ]/[AA] = 1.25). Solvent: bidistilled water

Modified PAA displayed similar traits to the pristine polymer in terms of solubility, that is, HQ-PAA was soluble in polar solvents, such as water, methanol, dioxane, THF, and DMF and defied solubility in non-polar organic solvents.

Analyses by UV-visible, FT-IR, XRD, SEM, and ^{13}C NMR (Figs. 1, 2, 3, 4, 5) certified the success of chemical modifications of PAA with HQ. UV-visible spectrum of HQ-PAA (Fig. 1) reveals a new absorption band at $\lambda_{\text{max}} = 288 \text{ nm}$, a featuring band of a hydroquinone unit. In addition, the infrared analysis (Fig. 2) came up with new absorption bands for HQ-PAA compared with those of virgin PAA. As can be clearly seen, it seems that the incorporation of HQ units onto PAA matrix has helped resolving its FT-IR spectrum, hinting at a high and regular substitution. The characteristic bands of the HQ entity appeared clearly as: (1) bands at around $1500\text{--}1550 \text{ cm}^{-1}$,

assigned to the aromatic C=C stretching; (2) two sharper bands at $860\text{--}870$ and $1200\text{--}1250 \text{ cm}^{-1}$, attributable to the angular deformation of C=C and the stretching of C–O, respectively; (3) a band at $1400\text{--}1425 \text{ cm}^{-1}$, assigned to planar C–H band of the benzene ring; and (4) a wide band at around 3400 cm^{-1} , ascribed to O–H band.

The analysis by ^{13}C NMR spectroscopy further supported the success of the chemical modification of poly(acrylic acid) (Fig. 3). Indeed, besides the chemical shifts of different carbons of PAA appearing at around of 36–42, 44–54, and 178–180 ppm, those of the HQ units are 112–116, 130, and 150 ppm.

Figure 4 illustrates the XRD patterns of PAA and HQ-PAA, indicating amorphous structures for both polymers as reported by other workers [26]. In the diffractogram of HQ-PAA, new peaks at 2θ equal to 27, 32, and 45° appeared, suggesting that a degree of crystallinity was ensued. Our results are consistent with the reported ones [27], confirming the grafting of HQ in the structure of the modified PAA.

SEM images of PAA and HQ-PAA are depicted in Fig. 5. The texture of PAA (Fig. 5a) is relatively flat and smooth, compared to that of HQ-PAA (Fig. 5b, c) which shows roughened surfaces filled with needles. This change proved the grafting of HQ within the PAA chains.

Surprisingly, the average molecular weight (Fig. 6; Table 1) of HQ-PAA was nearly unchanged or slightly lower than that of the starting PAA. Indeed, M_w of the modified HQ_x-PAA (x, a degree of substitution equal to 32 %) was estimated as $2.38 \times 10^6 \text{ g mole}^{-1}$ against $2.54 \times 10^6 \text{ g mole}^{-1}$ for PAA; that is, the mass of the modified polymer was about 1.06 times lower than the initial molecular weight of PAA, suggesting a degradation

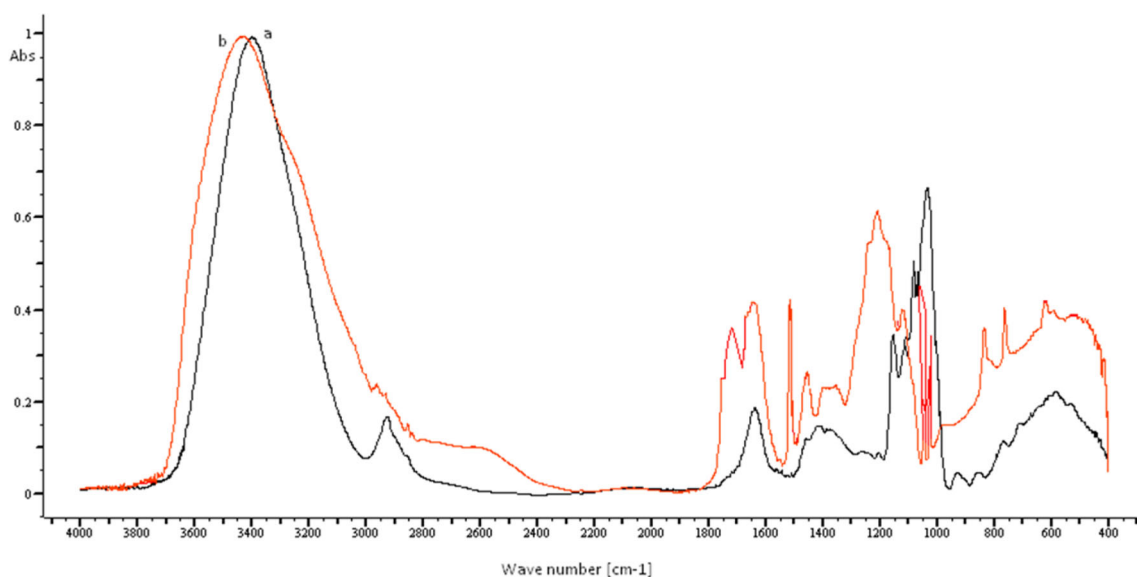


Fig. 2 FT-IR spectra: **a** PAA; **b** HQ-PAA ([BQ]/[AA] = 1.25)

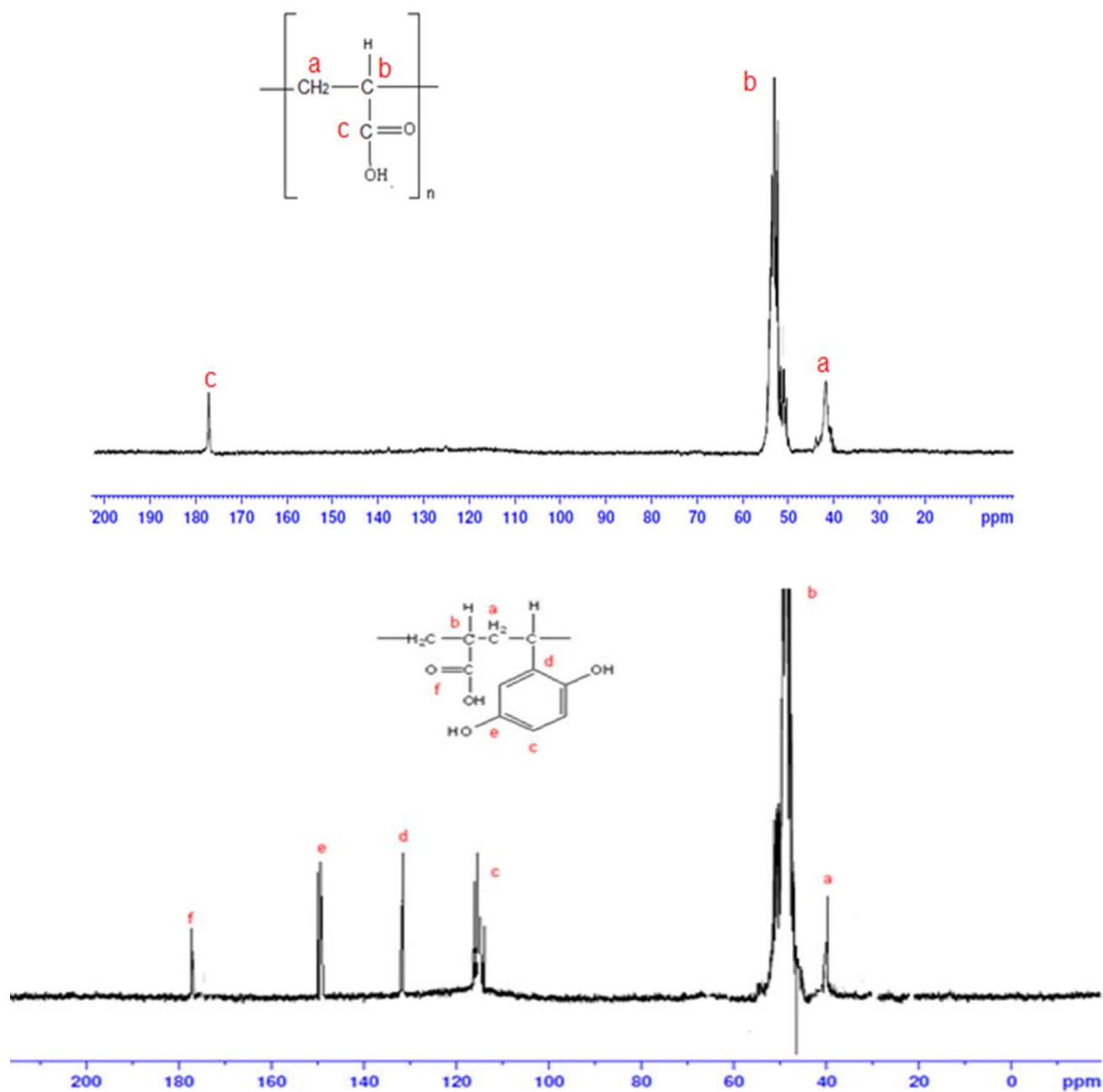


Fig. 3 ^{13}C NMR spectra of PAA and **HQ**-PAA. CD_3OD as a solvent

occurrence in the course of the modification reaction. This phenomenon was also observed earlier upon the reaction of PAA and PAAM (polyacrylamide) with 2,5-dihydroxybenzoquinone (DHBQ) under identical conditions [5, 13]. Neira et al. [28] reported the degradation of PAA when grafted onto cellulose using Fenton's reagent ($\text{Fe(II)}/\text{H}_2\text{O}_2$), a redox system.

The glass transition temperature for the modified PAA ($T_g = 135.8\text{ }^\circ\text{C}$) was lower than that for the pristine PAA ($151.26\text{ }^\circ\text{C}$), as noticed in Fig. 7 (Table 1). The lower T_g measured for **HQ**-PAA can be due to the relatively low

molecular weight obtained. The DSC thermogram of **HQ**-PAA revealed another thermal transition at $212.8\text{ }^\circ\text{C}$ which could be taken as the melting point T_m of the modified PAA. The small area at this endothermic peak would hint at the degree of crystallinity ensued during such functionalization as discussed above.

Thermogravimetric analyses of PAA and **HQ**-PAA are presented in Fig. 8. A two-step degradation for PAA can be noticed; an intense degradation of PAA (about 71 % weight loss) occurred between 250 and $300\text{ }^\circ\text{C}$, followed by a weaker one between 360 and $460\text{ }^\circ\text{C}$ (about 25 %

Fig. 4 XRD spectra of PAA and HQ-PAA ([BQ]/[AA] = 1.25)

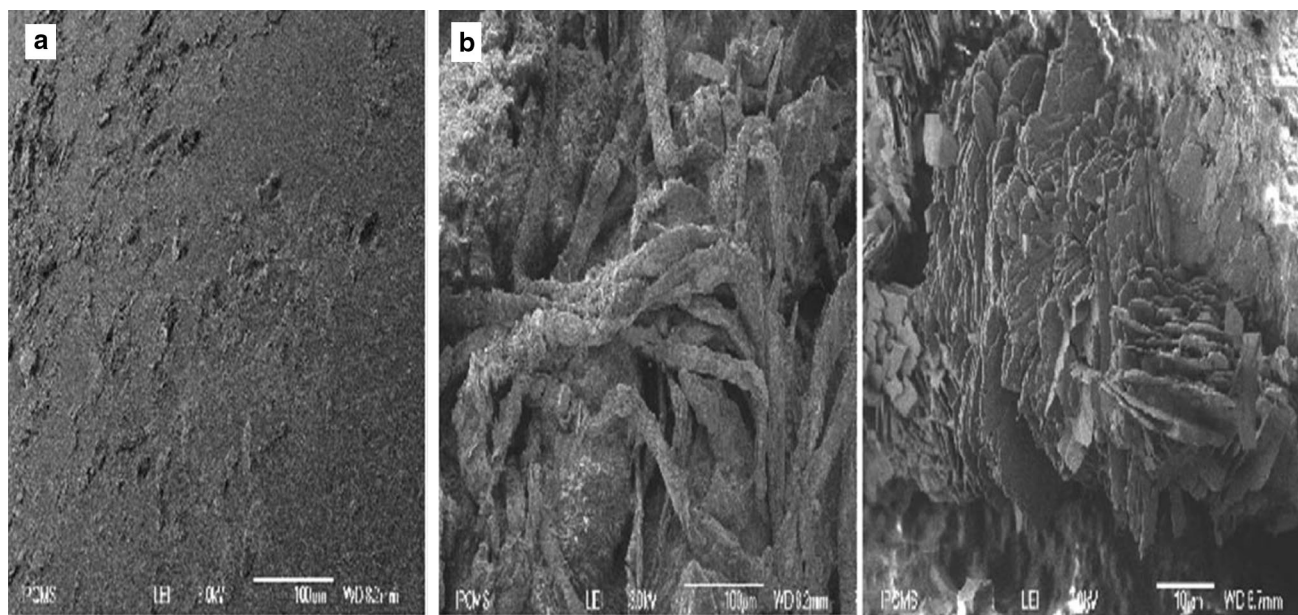
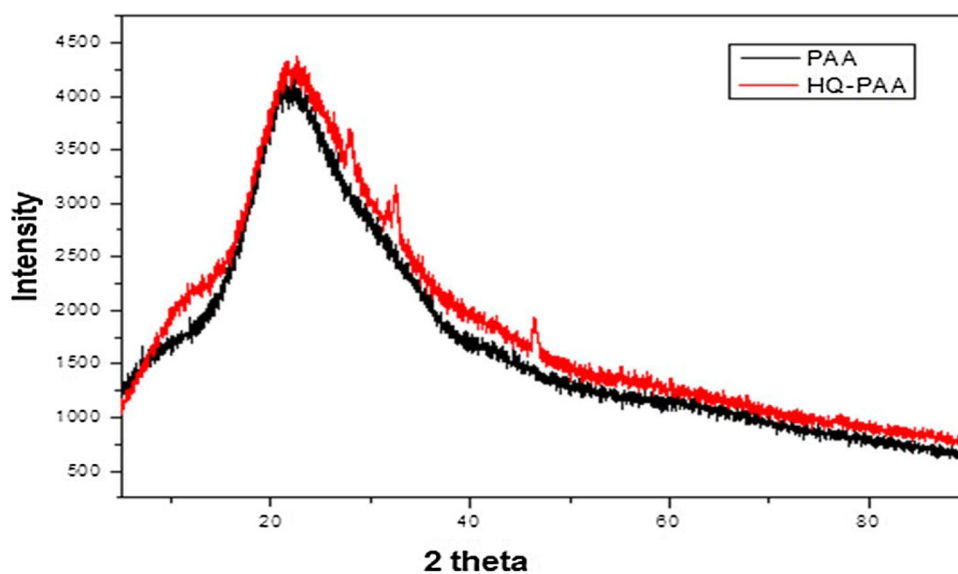


Fig. 5 SEM images: **a** PAA, $\times 230$; **b** HQ-PAA, $\times 230$; **c** HQ-PAA, $\times 1500$

weight loss). However, a three-stage degradation of HQ-PAA was detected; the first stage (10 %) started at 100 °C and continued up to 160 °C, the second (35 % weight loss) between 200 and 280 °C, and the third (31 % weight loss) began at 360 °C and continued to 440 °C. Three maximum loss rates manifested at 230, 403, and 131 °C; the first loss rate may be attributed to the decarboxylation or anhydride formation, and the second and the third loss rates may be assigned to the degradation of HQ moieties. The results obtained by TGA for HQ-PAA and PAA were consistent with those revealed by DSC measurements.

Effect of [BQ]/[monomer unit] ratio

The effect of [modifier]/[monomer unit] molar ratio, [BQ]/[AA], on substitution extent of the modification of PAA was assessed at 70–80 °C and for two reaction times, 3 and 6 h. Such an effect is illustrated in Fig. 9. The degree of modification was estimated by UV absorbance of the HQ-PAA using a calibration curve that was established by measuring the absorbance of dilute hydroquinone solutions at $\lambda_{\max} = 288$ nm; as can be noticed in the figure, the variations of modification degree increased with increasing



Fig. 6 GPC elution profiles for PAA and HQ-PAA ([BQ]/[AA]) = 1.25

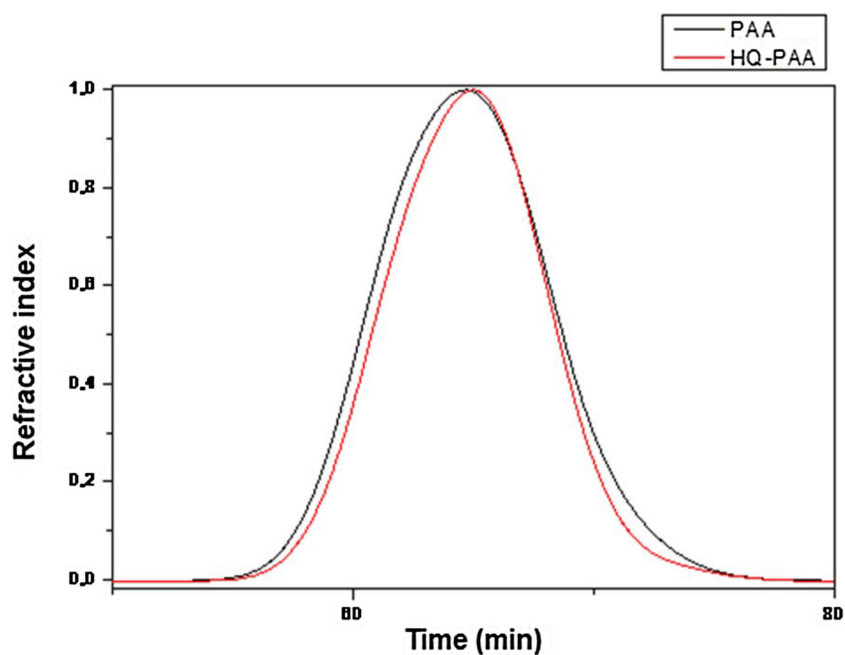


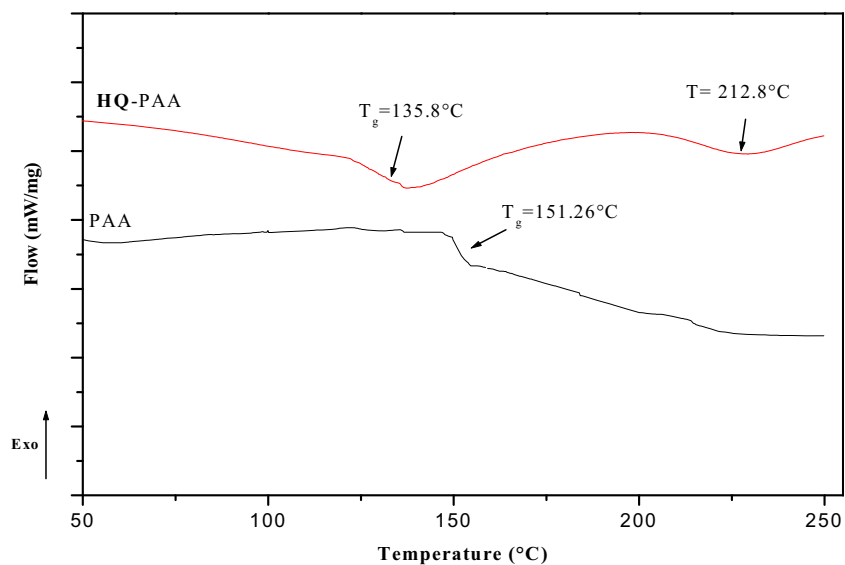
Table 1 Molecular weights of PAA, HQ-PAA, and their T_g

	$M_w \times 10^{-6}$ (g mol ⁻¹)	$M_n \times 10^{-6}$ (g mol ⁻¹)	M_w/M_n	T_g (°C)
PAA	2.54	1.45	1.75	151.26 (142) ^b
HQ-PAA ^a	2.38	1.51	1.58	135.8

^a Modified PAA using [BQ]/[AA] = 1.25

^b Reference [10]

Fig. 7 DSC thermograms of PAA and HQ-PAA ([BQ]/[AA]) = 1.25. Scanning rate: 5 °C/min; N₂ atmosphere



[BQ]/[AA] and high substitution extents (29–32 %) were gained with a ratio higher than 1. In addition, prolonging the reaction time from 3 to 6 h in both the cases did not improve significantly the substitution extent.

Effect of reaction time

The impact of reaction time on the modification extent of PAA for a [BQ]/[AA] ratio of 1.25 is presented in Fig. 10.

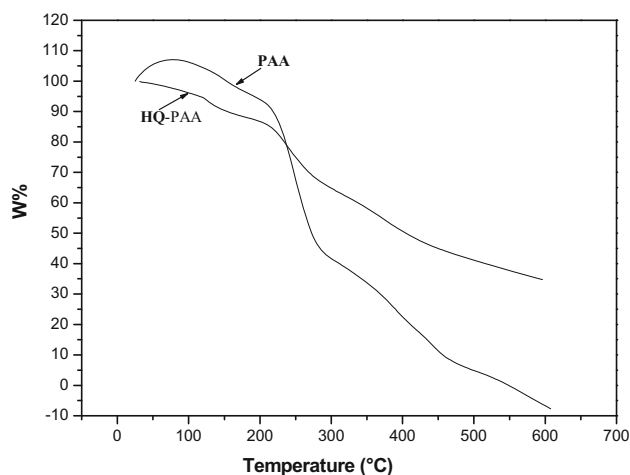


Fig. 8 TGA thermograms of PAA and **HQ-PAA** ([BQ]/[AA]) = 1.25. Heating rate: 10 °C/min; N₂ atmosphere

The substitution extent increased with increasing reaction time, and optimal substitutions were reached at a time of 5 h and leveled off at 32 % beyond this time.

Metallic adsorption–desorption study

PAA and **HQ-PAA** adsorbents were set by cross-linking their corresponding soluble polymers applying the oxidative decarboxylation conditions of Minisci as traced in Eqs. 4 and 5. The **HQ-PAA** used in the adsorption of the metallic ions was the one modified with a molar ratio [BQ]/[AA] of 1.25 that corresponds to 32 % degree of substitution. The effects of pH, time, ionic strength, temperature, adsorbent mass, and initial concentration of copper, on the

Cu(II) adsorption capacities of the PAA and **HQ-PAA** resins, were assessed, and the results are illustrated in Figs. 11, 12, 13, 14, and 15, 16 and compiled in Tables 2, 3, 4, and 5. A tentative structure of the **HQ-PAA** adsorbent/Cu²⁺ complex at pH of 5.4 is pictured in Fig. 11.

It can be seen that the adsorption capacities of the PAA and **HQ-PAA** resins with respect to copper (II) increased with increasing pH and time, as shown in Figs. 12 and 13. They remained constant beyond a time of about 3 h. At pH values lower than 3, the sorption rate increased by raising the pH, but at higher values, the rate was independent on pH. The impact of this parameter on the removal of metallic ions from solutions is clear, because it affects the surface charge of sorbent. A higher pH would favor the tendency of negative charge formation on the sorbent, leading to an increase in the electrostatic attraction between the positively charged metallic ions and the negatively charged sorbent, thus a greater metallic sorption. The capacity exchanges were found to be 3.58 and 17.17 mg g⁻¹, respectively, at an optimal pH of 5.4 and a time of 3 h. Hence, **HQ-PAA** resin was nearly five times more effective than PAA resin in terms of copper (II) adsorption. This finding can be attributed to the grafted **HQ** moieties on the PAA matrix. The experiment was limited to the indicated pH values, because copper hydroxide would precipitate at pH values higher than 5.4, and would interfere with the actual results. On the other hand, the removal efficiency of metallic ion was found unexpectedly unaffected by increasing the ion strength of the solution, as shown in Fig. 14 and Table 2. In fact, the addition of NaNO₃, as an electrolyte, at varying

Fig. 9 Plot of the variation of substitution degree of PAA, *S* (%), as a function of [BQ]/[AA] molar ratio. Temperature = 70–80 °C

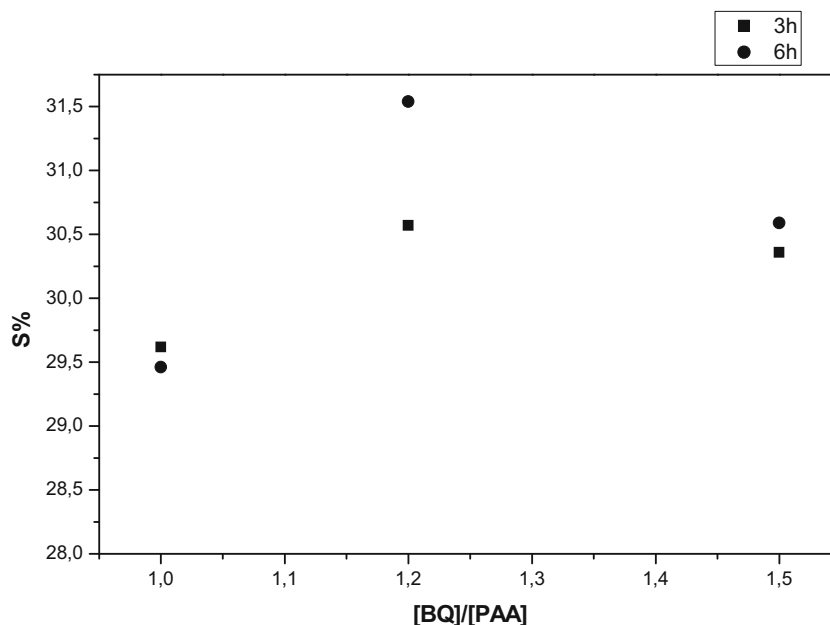


Fig. 10 Variation of the substitution degree of PAA, S (%), as a function of time. $T = 70\text{--}80\text{ }^{\circ}\text{C}$

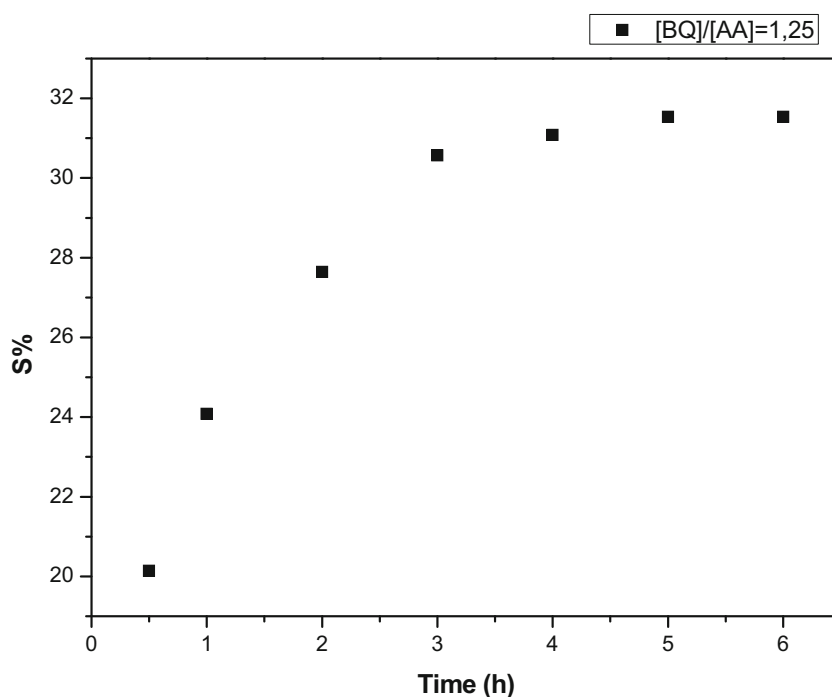
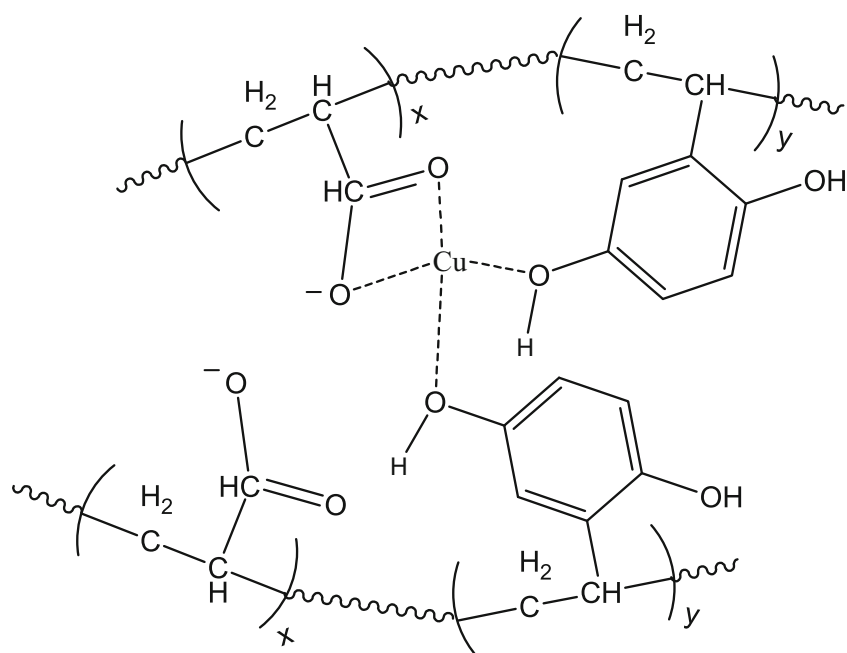


Fig. 11 Proposed structure of the copper (II)/HQ-PAA complex at pH 5.4



concentrations neither improved nor declined the sorption property. The present results are in good agreement with those reported [29, 30].

The effect of temperature on the adsorption capacities of the resins is shown in Fig. 15 and Table 3, demonstrating that the higher the temperature, the greater the adsorption capacity; at optimal pH (5.4) and time (3 h), the exchange capacities were 5.5 and 20.25 mg g⁻¹ at a temperature of 45 °C for PAA and HQ-PAA resins, respectively. In these

conditions, the COOH groups in the adsorbing resins are in the form of carboxylate ions, because the working pH (5.4) is higher than pK_a of PAA (4.7), and the phenolic OH groups in the HQ-PAA resin are not ionized due to their higher pK_a (~9.4); the carboxylate ions would complex metallic ions more favorably than the catechol hydroxyl groups.

Figures 16 and 17 picture the effects of the adsorbing resin mass and the initial copper concentration on the

Fig. 12 Variations of adsorption capacity Q_t of PAA resin for copper (II) as a function of time and pH.

$V = 50$ mL, $C_0 = 50$ mg/L, $W = 0.1$ g, $[\text{NaNO}_3] = 0$, and $T = 30$ °C

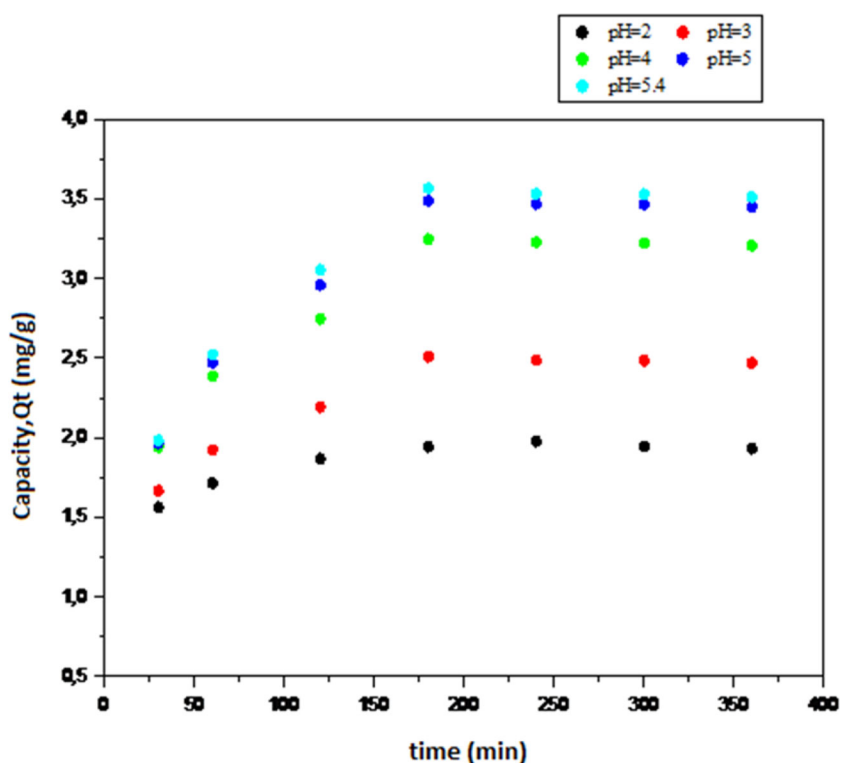
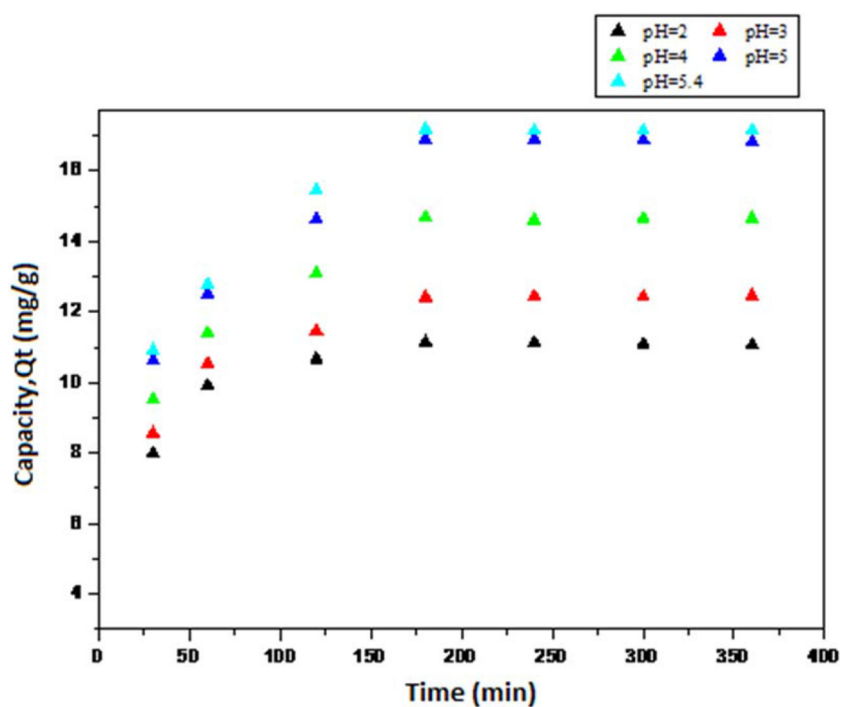


Fig. 13 Variations of adsorption capacity Q_t of HQ-PAA resin ($[\text{BQ}]/[\text{AA}] = 1.25$) for copper (II) as a function of time and pH. $V = 50$ mL,

$C_0 = 50$ mg/L, $W = 0.1$ g, $[\text{NaNO}_3] = 0$, and $T = 30$ °C



sorption of copper ion Cu(II), and the results are compiled in Tables 4 and 5. As can be noticed in Table 4, about 94 % enhancement of the exchange capacity of PAA resin was observed at optimal conditions by increasing the mass of the sorbent by twofold, but only 22 % enhancement for

HQ-PAA resin was found. Raising the initial concentration of copper nitrate improved the metal ion uptakes of the resins (Table 5) with nearly the same extents as with the variation of sorbent mass. These results are in tune with the published reports [31, 32].



Fig. 14 Variations of adsorption capacity Q_t of HQ-PAA resin ($[BQ]/[AA] = 1.25$) for copper (II) as a function of time and $[\text{NaNO}_3]$. $V = 50$ mL, $C_0 = 50$ mg/L, $W = 0.1$ g, pH 5.4, and $T = 30$ °C

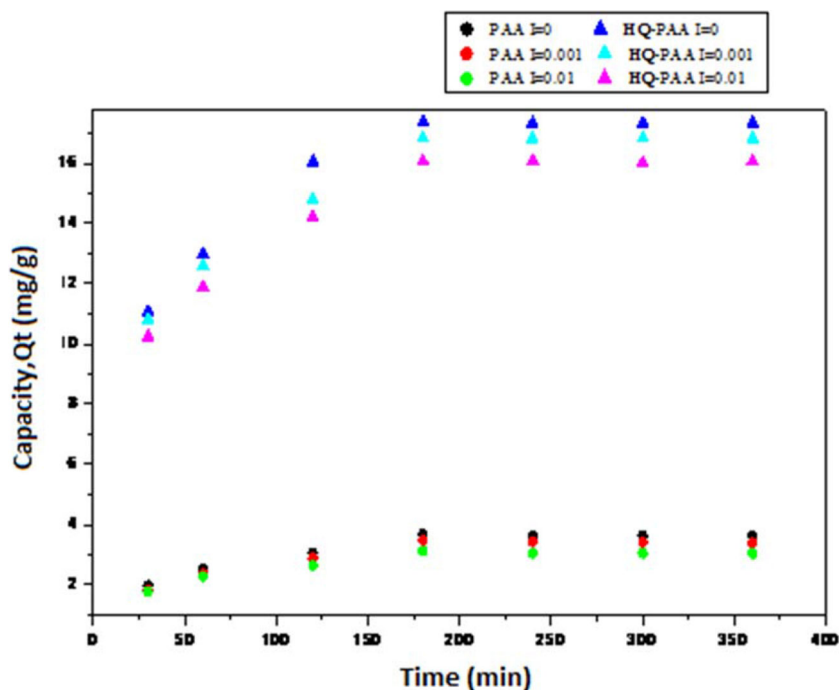
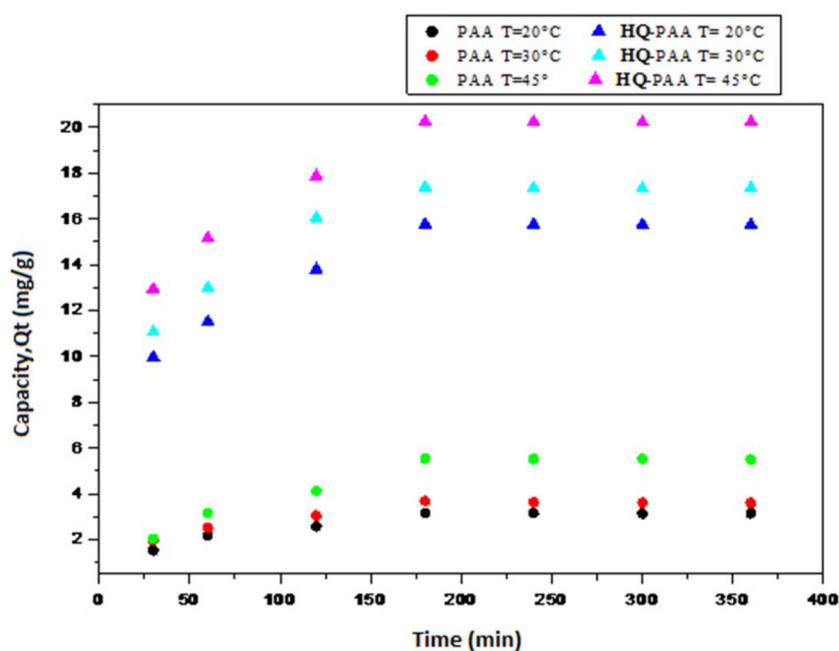


Fig. 15 Variations of adsorption capacity Q_t of HQ-PAA ($[BQ]/[AA] = 1.25$) and PAA resins for copper (II) as a function of time and temperature. $V = 50$ mL, $C_0 = 50$ mg/L, $W = 0.1$ g, $[\text{NaNO}_3] = 0$, $T = 30$ °C, and pH 5.4



The adsorption of lead (II) and cadmium (II) by the resins was conducted and compared with that of copper (II) under the same optimal conditions. The adsorption capacities of the resins towards these metal ions are depicted in Fig. 18 and gathered in Table 6. Maximum adsorptions of Pb(II) and Cd(II) by PAA resin were 7.04 and 2.88 mg g⁻¹, and were 20.84 and 12.69 mg g⁻¹ by HQ-PAA resin. Under the actual experimental conditions, the exchange capacity is in this order: Pb(II) > Cu(II) > Cd(II). The adsorption

capacity of the adsorbent is more for lead when compared to other metals, because the stability constants of complexes of lead with carboxylates and phenols are greater than those for other metals [33, 34]. The cross-linked poly(acrylic acid-co-Kryptofix-22-DM) [36], the tetrahydroxybenzene-functionalized PAA [5], and the tetrahydroxybenzene-functionalized PAAm [14] showed the same order of sorption capacity. Overall, our results are within with those reported in the literature (Table 7).

Fig. 16 Variations of adsorption capacity Q_t of HQ-PAA resin ($[BQ]/[AA] = 1.25$) for copper (II) as a function of adsorbent mass. $V = 50$ ml, $C_0 = 50$ mg/L, pH 5.4, and $T = 30$ °C

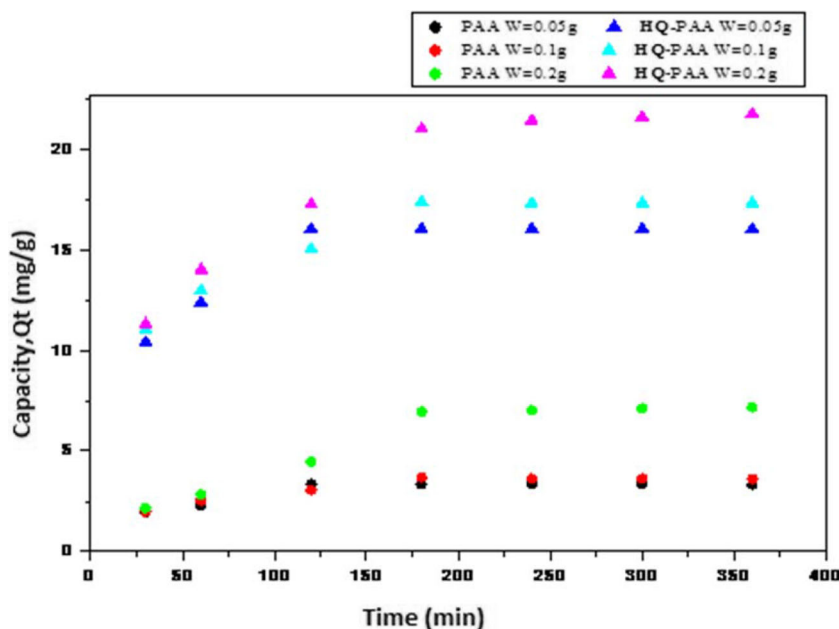


Table 2 Sorption of copper ion at different $[NaNO_3]$

$[NaNO_3]$	Sorption of Cu^{2+} (mg g ⁻¹)	
	PAA	HQ-PAA ^a
0	3.58	17.17
0.001	3.46	16.81
0.01	3.11	16.01

pH 5.4; $t = 3$ h; $C_0 = 50$ mg/L; $T = 30$ °C; $W = 0.1$ g

^a Modified PAA using $[BQ]/[AA] = 1.25$

Table 3 Sorption of copper ion at different temperatures

Temperature (°C)	Sorption of Cu^{2+} (mg g ⁻¹)	
	PAA	HQ-PAA ^a
20	3.17	15.76
30	3.58	17.17
45	5.54	20.25

pH 5.4; $t = 3$ h; $W = 0.1$ g; $[NaNO_3] = 0$ g/L; $C_0 = 50$ mg/L; $T = 30$ °C

^a Modified PAA using $[BQ]/[AA] = 1.25$

Adsorption kinetics

Pseudo-first-order model (Lagergren equation) The pseudo-first-order kinetic is expressed, as shown in Eq. 8 [37]:

$$\log(Q_e - Q_t) = \log Q_e - \frac{k_1 t}{2.303} \tag{8}$$

where

Table 4 Sorption of copper ion at different sorbent masses

Sorbent mass (g), W	Sorption of Cu^{2+} (mg g ⁻¹)	
	PAA	HQ-PAA ^a
0.05	3.32	15.06
0.10	3.58	17.17
0.20	6.94	21.03

pH 5.4; $t = 3$ h; $C_0 = 50$ mg/L; $[NaNO_3] = 0$ g/L

^a Modified PAA using $[BQ]/[AA] = 1.25$

k_1 is the pseudo-first-order rate constant (min⁻¹), Q_e is the adsorption capacity of the adsorbent (mg g⁻¹), Q_t is the amount of Cu ion adsorbed at time t (mg g⁻¹), where k_1 is computed from the slope of the plot of $\ln(Q_e - Q_t)$ versus t (Fig. 19).

Pseudo-second-order model (Ho-McKay equation) The pseudo-second-order kinetic is expressed as shown in Eq. 9 [38].

$$t/Q_t = t/Q_e + 1/k_2 Q_e^2 \tag{9}$$

where k_2 is the pseudo-second-order rate constant (g mg⁻¹ min⁻¹) and computed from the slope of the plot of t/Q_t versus t (Fig. 20).

The results of the applied models to the copper (II) adsorption by PAA and HQ-PAA are illustrated in Figs. 19 and 20 and compiled in Table 8. As can be noticed in Table 8, the experimental Q_e values are so distant from the calculated ones and the correlation coefficients are low, suggesting that this adsorption does not obey a pseudo-first kinetic model; the graphs in Fig. 19 are not straight lines,

Table 5 Sorption of copper ion at different Cu^{2+} concentrations

Initial concentration of copper (II), C_0 (mg/L)	Sorption of Cu^{2+} ($mg\ g^{-1}$)	
	PAA	HQ-PAA ^a
10	3.23	15.89
50	3.58	17.17
100	6.77	20.84

pH 5.4; $t = 3\ h$; $W = 0.1\ g$; $[NaNO_3] = 0\ g/L$

^a Modified PAA using $[BQ]/[AA] = 1.25$

Fig. 17 Variations of adsorption capacity Q_t of HQ-PAA resin ($[BQ]/[AA] = 1.25$) for copper (II) as a function of $Cu(II)$ concentration. $V = 50\ mL$, pH 5.4, $T = 30\ ^\circ C$, and $W = 0.1\ g$

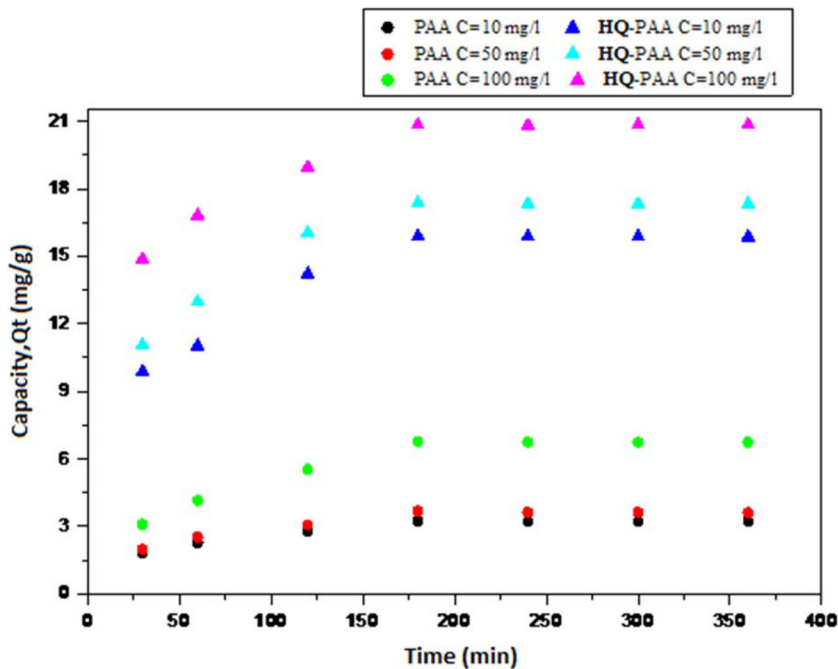
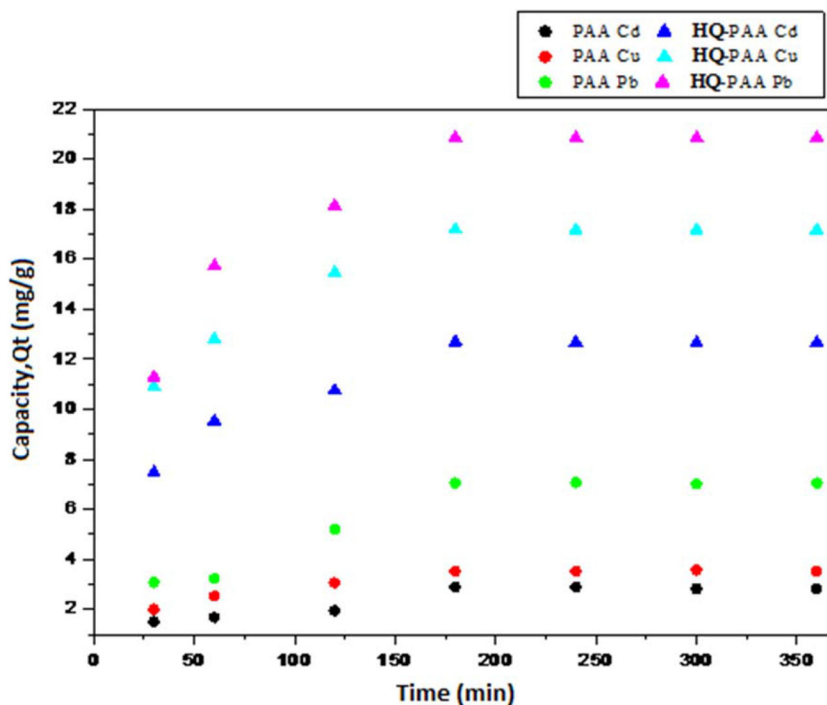


Fig. 18 Variations of adsorption capacities Q_t of HQ-PAA ($[BQ]/[AA] = 1.25$) and PAA resins for copper (II), lead (II), and cadmium (II) as a function of time. $V = 50\ mL$, $C_0 = 50\ mg/L$, $W = 0.1\ g$, $[NaNO_3] = 0$, $T = 30\ ^\circ C$, and pH 5.4



precluding the validity of Lagergren equation. However, the straight lines of the plot t/Q_t versus time (Fig. 20) are indicative of the validity of Ho-McKay equation; indeed, the experimental Q_e values and the calculated ones are so close and the correlation coefficients are high as shown in Table 8, suggesting that the adsorption fits well a pseudo-second kinetic model.

Adsorption isotherms

Three adsorption isotherms models were examined for our data on the copper adsorption by PAA and HQ-PAA: Freundlich, Langmuir, and Temkin.

Freundlich isotherm The linear form of the Freundlich equation is given in Eq. 10 [39]. For Freundlich isotherm, the ratio of sorbate adsorbed onto a given mass of adsorbent to the sorbate concentration in solution is not constant:

$$\log Q_e = \log K_F + (1/n) \log C_e \quad (10)$$

where

Q_e is the amount of solute adsorbed per-unit weight of adsorbent (mg g^{-1}),

K_F is the Freundlich constant (mg g^{-1}),

C_e is the equilibrium concentration of the solute in the bulk solution (mg L^{-1}),

$1/n$ is the heterogeneity factor indicating the adsorption intensity.

Table 6 Sorption of Pb^{2+} , Cu^{2+} , and Cd^{2+}

Metallic ions	Sorption of ions (mg g^{-1})	
	PAA	HQ-PAA ^a
Pb^{2+}	7.04	20.84
Cu^{2+}	3.58	17.17
Cd^{2+}	2.88	12.69

pH 5.4; $t = 3$ h; mass of resin $W = 0.1$ g; $[\text{NaNO}_3] = 0$ g/L

^a Modified PAA using $[\text{BQ}]/[\text{AA}] = 1.25$

Langmuir isotherm The linear form of Langmuir isotherm equation is given in Eq. 11 [40]. For the Langmuir isotherm, a monomolecular layer is supposedly formed, as the sorbate molecules are adsorbed without any interactions between them:

$$C_e/Q_e = (1/Q_{\max}K_L) + (C_e/Q_{\max}) \quad (11)$$

where

Q_{\max} is the maximum adsorption capacity of the adsorbent (mg g^{-1}),

K_L is the Langmuir adsorption constant (L mg^{-1}).

Temkin isotherm The linear form of the Temkin model equation is given in Eq. 12 [41]. For the Temkin model theory, the effect of the interactions between sorbate molecules on adsorption isotherms is taken into account, suggesting that the heat of adsorption of all the molecules in the layer would decrease linearly:

$$Q_e = B \ln A + B \ln C_e \quad (12)$$

where

$B = RT/b_T$, b_T is the Temkin constant related to heat of sorption (J mol^{-1}), R the gas constant (8.314 J/mol K), and T is the absolute temperature,

A is the Temkin isotherm constant (L g^{-1}).

Data of the study of adsorption isotherms are illustrated in Figs. 21, 22, and 23, and Table 9. Based on the correlation coefficient R^2 , none of the examined isotherm models would fit the adsorption data in the case of PAA; indeed, R^2 is poorly low and is in the range of 0.40–0.76. However, in the case of HQ-PAA, the three models are more favorable; yet, the Langmuir model ($R^2 = 0.993$) fits better than Temkin ($R^2 = 0.918$) and Freundlich ($R^2 = 0.816$). The fact that the present data obey better to Langmuir model can be assigned to the homogenous distribution of active sites on the HQ-PAA surface, as the Langmuir equation assumes a homogenous surface, where all the sites have equal adsorption energies. The Langmuir

Table 7 Adsorption capacity (mg g^{-1}) of some polyhydroxybenzene-functionalized resins towards Cu^{2+} , Cd^{2+} , and Pb^{2+}

Polymer	Functionalizing group	Cu^{2+}	Cd^{2+}	Pb^{2+}	References
		(mg g^{-1})	(mg g^{-1})	(mg g^{-1})	
Cellulose	1,2-Dihydroxybenzene (catechol)	11.83	13.00	21.5	[34]*
Amberlite XAD-4	1,2-Dihydroxybenzene (catechol)	5.69	2.89	/	[33]*
Poly(vinylcatechol-co-divinylbenzene)	1,2-Dihydroxybenzene (catechol)	6.44	9.10	/	[35]*
Poly(acrylic acid)	1,2,4,5-Tetrahydroxybenzene (benzene-1,2,4,5-tetrol)	19.54	14.90	22.16	[5]
Polyacrylamide	1,2,4,5-Tetrahydroxybenzene (benzene-1,2,4,5-tetrol)	18.87	17.58	20.74	[13]
Polyacrylamide	1,4-Dihydroxybenzene (hydroquinone)	5.01	4.36	5.91	[14]
Poly(acrylic acid)	1,4-Dihydroxybenzene (hydroquinone)	17.17	12.69	20.84	Present work

* The mentioned values were computed from the results given in the corresponding articles

Fig. 19 Pseudo-first-order model fit for the adsorption of Cu^{2+} at pH 5.4: **a** PAA; **b** HQ-PAA

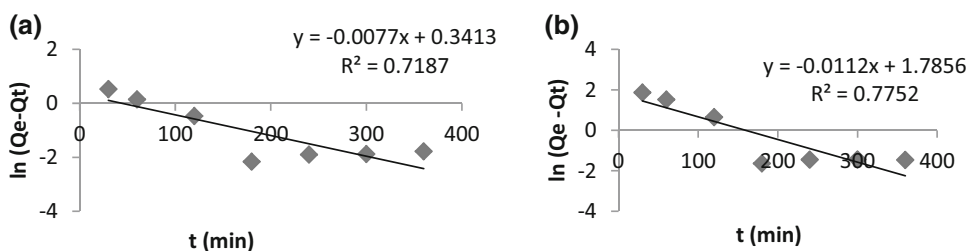


Fig. 20 Pseudo-second-order model fit for the adsorption of Cu^{2+} at pH 5.4: **a** PAA; **b** HQ-PAA

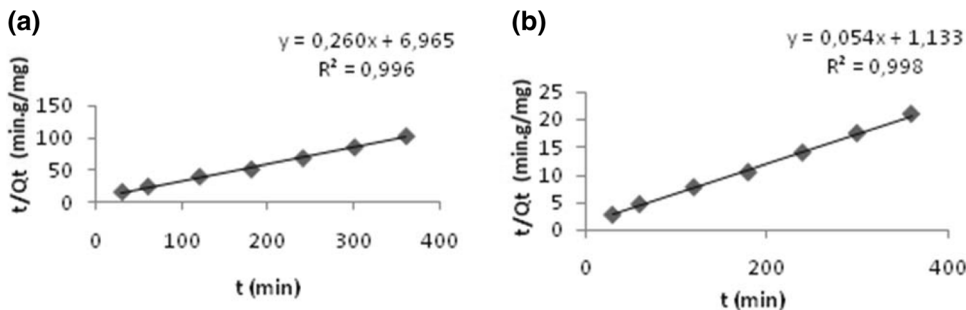
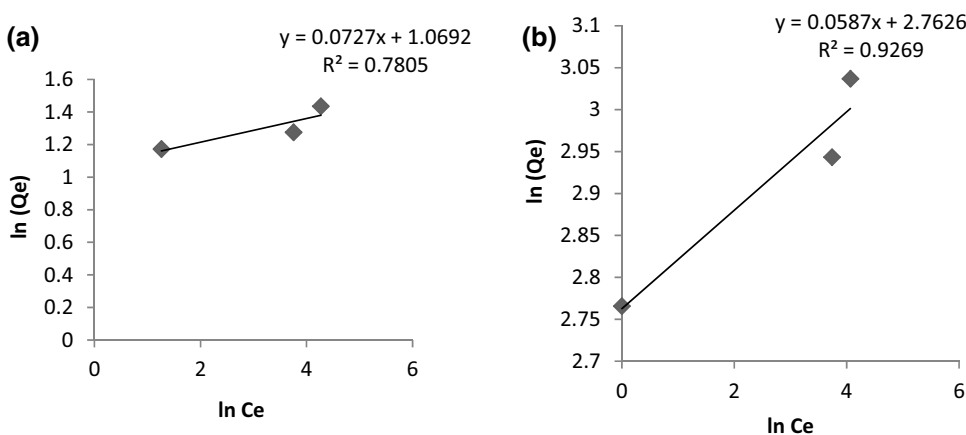


Table 8 Results of pseudo-first- and second-order models of Cu^{2+} adsorption

Sorbent	Pseudo-first-order model				Pseudo-second-order model			
	$Q_{e \text{ exp}}$ (mg g^{-1})	$Q_{e \text{ cal}}$ (mg g^{-1})	k_1 (min^{-1})	R^2	$Q_{e \text{ exp}}$ (mg g^{-1})	$Q_{e \text{ cal}}$ (mg g^{-1})	k_2 ($\text{g mg}^{-1} \text{min}^{-1}$)	R^2
PAA	3.58	1.41	0.017	0.718	3.58	3.84	0.01	0.996
HQ-PAA	17.17	5.96	0.025	0.775	17.17	18.34	0.002	0.998

Fig. 21 Plots of Freundlich model for Cu^{2+} adsorption: **a** PAA; **b** HQ-PAA



constant K_L is 0.181 L mg^{-1} , a value lower than 1, indicating favorable adsorption. The maximum adsorption capacity of the HQ-PAA adsorbent, Q_{max} , was measured to be 22.37 mg g^{-1} . The Freundlich treatment of our data afforded $1/n$ values greater than 1, suggesting that the Cu^{2+} adsorption onto HQ-PAA adsorbent was unfavorable under the studied experimental conditions.

Thermodynamic adsorption parameters

To acquire an insight into the adsorption process of the Cu^{2+} ions and its distribution between the adsorbent and the aqueous medium, thermodynamic factors of the whole process are eagerly sought for; the Gibbs free energy of adsorption (ΔG^0), the entropy of adsorption (ΔS^0), and the

Fig. 22 Plots of Langmuir model for Cu^{2+} adsorption: **a** PAA; **b** HQ-PAA

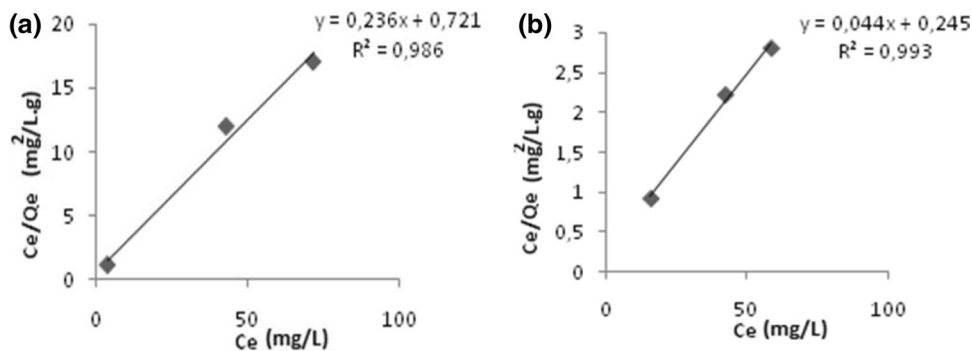


Fig. 23 Plots of Temkin model for Cu^{2+} adsorption: **a** PAA; **b** HQ-PAA

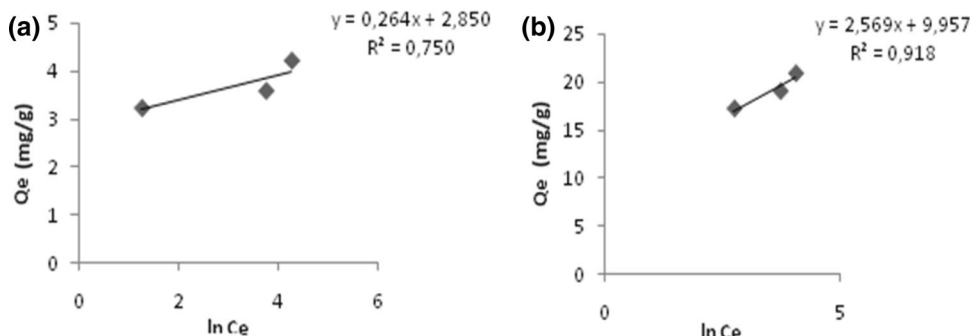
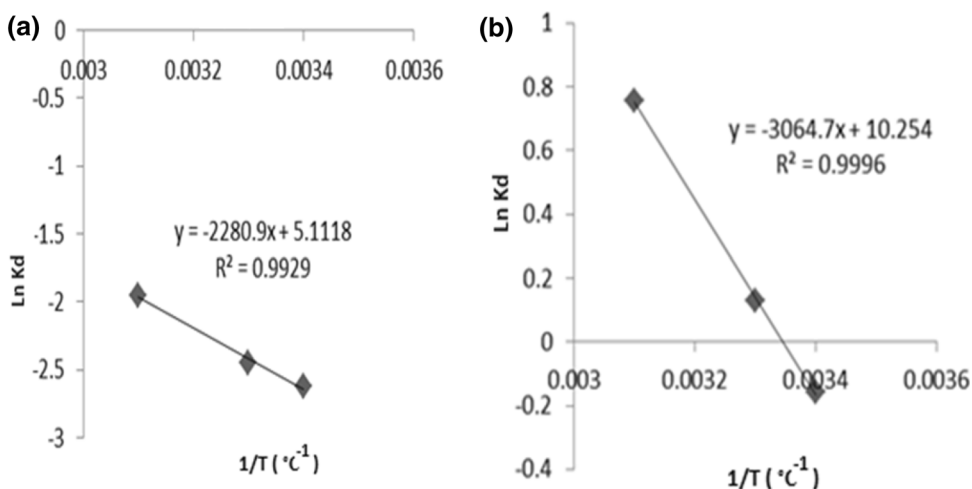


Table 9 Parameters of adsorption isotherm models for Cu^{2+} /PAA and Cu^{2+} /HQ-PAA systems

Sorbent	Freundlich			Langmuir			Temkin		
	$1/n$	K_f (mg g^{-1})	R^2	Q_{max} (mg g^{-1})	K_L (L mg^{-1})	R^2	A (L g^{-1})	B (J mol^{-1})	R^2
PAA	6.514	2.512	0.480	6.157	0.067	0.762	19.995	0.690	0.407
HQ-PAA	17.301	15.559	0.816	22.37	0.181	0.993	48.233	1.037	0.918

Fig. 24 Plots of $\ln K_d$ versus $1/T$. **a** PAA; **b** HQ-PAA



enthalpy of adsorption (ΔH^0) can be computed from the following equations (Eqs. 13–15). ΔH^0 and ΔS^0 were taken as slopes and intercepts of the plot of $\ln K_d$ versus $1/T$ (Fig. 24), respectively. The results are gathered in

Table 10. The positive value of enthalpy ΔH^0 indicates that the adsorption is an endothermic process, and the positive value of entropy ΔS^0 is attributed to an occurrence of a less ordered molecular arrangement of both carboxylate ion and

Table 10 Thermodynamic parameters of the adsorption of Cu^{2+}

Sorbent	T (°C)	$1/T$ (K^{-1})	$\ln K_d$	ΔG^0 (kJ mol^{-1})	ΔH^0 (kJ mol^{-1})	ΔS^0 ($\text{J mol}^{-1} \text{K}^{-1}$)	R^2
PAA	20	0.0034	-2.620	6.382	18.96	42.49	0.992
	30	0.0033	-2.448	6.166			
	45	0.0031	-1.947	5.147			
HQ-PAA	20	0.0034	-0.158	0.384	25.47	85.25	0.999
	30	0.0033	0.130	-0.327			
	45	0.0031	0.757	-2.001			

Table 11 Adsorption–desorption results

Metal ion	Cycle	Amount of ion adsorbed (mg)		Amount of ion desorbed (mg)		DP (%)	
		PAA	HQ-PAA ^a	PAA	HQ-PAA ^a	PAA	HQ-PAA ^a
Pb^{2+}	1	6.98	20.82	6.85	20.59	98.16	98.91
	2	6.89	20.62	6.76	20.32	98.14	98.54
	3	6.86	20.52	6.73	20.19	98.07	98.41
Cu^{2+}	1	3.52	17.17	3.46	16.92	98.20	98.54
	2	3.41	17.10	3.35	16.81	98.17	98.30
	3	3.38	16.85	3.30	16.55	97.58	98.19
Cd^{2+}	1	2.89	12.65	2.86	12.54	99.08	99.12
	2	2.86	12.60	2.83	12.47	98.94	99.02
	3	2.84	12.57	2.81	12.44	98.72	98.97

^a Modified PAA using $[\text{BQ}]/[\text{AA}] = 1.25$

hydroquinone unit [42]. Negative values of Gibbs free energy (ΔG^0) indicate a favorable and spontaneous adsorption. Worthy of note is that, at 20 °C, no adsorption took place as the value of ΔG^0 is positive. At a working temperature, that is 30 °C, adsorption occurred to a certain extent as ΔG^0 is $-0.327 \text{ kJ mol}^{-1}$; however, a more favorable and spontaneous adsorption could happen at 40 °C ($\Delta G^0 = -2.001 \text{ kJ mol}^{-1}$):

$$\Delta G^0 = -RT \ln K_d \quad (13)$$

$$\ln K_d = \frac{\Delta S^0}{R} - \frac{\Delta H^0}{RT} \quad (14)$$

$$K_d = \frac{C_0 - C_e}{C_e} \cdot \frac{V}{w} \quad (15)$$

where

- R is the ideal gas constant ($8.314 \text{ J mol}^{-1} \text{ K}^{-1}$),
- T is the absolute temperature (K),
- K_d is the equilibrium constant,
- C_e is the equilibrium metal ion concentration (mg L^{-1}).

Desorption performance

In the sake of reusability of the resin in adsorption of metals, the adsorption–desorption of metal ions was carried

out. The desorption of metal-adsorbed resins was accomplished by treatment with 0.1 N nitric acid at 30 °C. The results of adsorption–desorption of ions by the resins are gathered in Table 11. The results revealed that the capacity exchanges of the resins were retained even after three adsorption–desorption cycles for copper (II), lead (II), and cadmium (II) ions, hinting at the feasibility of reuse of the resins in the removal process. The desorption extents of these ions from PAA and HQ-PAA resins were substantially high and exceeding 98 %.

Conclusions

The application of oxidative decarboxylation of Minisci to the chemical modification of poly(acrylic acid) was successful. As expected, metallic adsorption of hydroquinone-grafted poly(acrylic acid) was greater than that of the virgin poly(acrylic acid). In addition, to achieve higher metal ion uptakes by poly(acrylic acid) and its modified resin, one needs to work under the following conditions: pH 5.4, time 180 min, and temperature 45 °C. Metallic adsorption by hydroquinone-modified poly(acrylic acid) resin occurred at temperatures of only higher than 30 °C. Finally, the adsorption–desorption results suggest the utilization of the



hydroquinone-modified poly(acrylic acid) as a cation exchange resin.

Open Access This article is distributed under the terms of the Creative Commons Attribution 4.0 International License (<http://creativecommons.org/licenses/by/4.0/>), which permits unrestricted use, distribution, and reproduction in any medium, provided you give appropriate credit to the original author(s) and the source, provide a link to the Creative Commons license, and indicate if changes were made.

References

- Francis S, Kumar M, Varshney L (2004) Radiation synthesis of superabsorbent poly(acrylic acid)-carrageenan hydrogels. *Rad Phys Chem* 69:481–486
- Hussain T, Ranjha NM, Shahzad Y (2011) Swelling and controlled release of tramadol hydrochloride from a pH-sensitive hydrogel. *Des Monom Polym* 14:233–249
- Adnadjevic B, Jovanovic J (2008) Novel approach in investigation of the poly(acrylic acid) hydrogel swelling kinetics in water. *J Appl Polym Sci* 107:3579–3587
- Moulay S, Boukherissa M, Abdoune F, Benabdelmoumene FZ (2005) Low molecular weight poly(acrylic acid) as a salt scaling inhibitor in oilfield operations. *J Iran Chem Soc* 2:212–219
- Bensacia N, Moulay S (2012) Functionalization of polyacrylic acid with tetrahydroxybenzene via a homolytic pathway: application to metallic adsorption. *Intern J Polym Mater* 61:699–722
- Adewuyi S, Ondigo DA, Zugle R, Tshentu Z, Nyokong T, Torto N (2012) A highly selective and sensitive pyridylazo-2-naphthol-poly(acrylic acid) functionalized electrospun nanofiber fluorescence “turn-off” chemosensory system for Ni²⁺. *Anal Meth* 4:1729–1735
- Müller M, Keßler B, Fröhlich J, Poeschla S, Torger B (2011) Polyelectrolyte complex nanoparticles of poly(ethyleneimine) and poly(acrylic acid): preparation and applications. *Polymers* 3:762–778
- Li D, Jiang Y, Li C, Wu Z, Chen X, Li Y (1999) Self-assembly of polyaniline/polyacrylic acid films via acid-base reaction induced deposition. *Polymer* 40:7065–7070
- Lu X, Yu Y, Chen L, Mao H, Wang L, Zhang W, Wei Y (2005) Poly(acrylic acid)-guided synthesis of helical polyaniline micro-wires. *Polymer* 46:5329–5333
- Moulay S, Mehdaoui R (2004) Hydroquinone/catechol-bearing polyacrylic acid: redox polymer. *React Funct Polym* 61:265–275
- Xu Y, Lin Y, Zhuang L, Lin J, Lv J, Huang Q, Sun J (2013) Bleomycin loaded magnetite nanoparticles functionalized by polyacrylic acid as a new antitumoral drug delivery system. *BioMed Res Intern*. 2013;Article ID 462589:5. doi:10.1155/2013/462589
- Sakaguchi Y, Nishino J, Tamaki K, Nagae T (1968) Preparation and potentiometric titration of several polymer carboxylic acids. *Kobunshi Kagaku* 25:761–768
- Moulay S, Bensacia N, Garin F, Fechete I, Boos A (2013) Polyacrylamide-based Sorbents for the removal of hazardous metals. *Adsorpt Sci Technol* 38:691–710
- Moulay S, Bensacia N, Garin F, Fechete I, Boos A (2014) Synthesis of polyacrylamide-bound hydroquinone via a homolytic pathway: application for removal of heavy metals. *CR Chim* 17:849–859
- Bertini F, Caronna T, Galli R, Minisci F, Porto O (1972) New processes for the homolytic alkylation of protonated heteroaromatic bases. *Chim Ind (Milan)* 54:425–426
- Bensacia N, Fechete I, Moulay S, Hulea O, Boos A, Garin F (2014) Kinetic and equilibrium studies of lead (II) adsorption from aqueous media by KIT-6 mesoporous silica functionalized with COOH. *CR Chim* 17:869–880
- Bensacia N, Fechete I, Moulay S, Debbih-Boustila S, Boos A, Garin F (2014) Removal of cadmium (II) from aqueous media using COOH/TUD-1 mesoporous solid. Kinetic and thermodynamic studies. *Environ Eng Manag J* 13:2675–2686
- Shah BA, Shah AV, Bhatt RR (2007) Studies of chelation ion-exchange properties of copolymer resin derived from salicylic acid and its analytical applications. *Iran Polym J* 16:173–184
- Bhatt RR, Shah BA (2015) Sorption studies of heavy metal ions by salicylic acid-formaldehyde-catechol terpolymeric resin: isotherm, kinetic and thermodynamics. *Arab J Chem* 8:414–426
- Moulay S, Mehdaoui R (2006) Poly(methacrylic acid)-bound dihydroxybenzene units: redox polymers. *J Appl Polym Sci* 100:954–961
- Kara A, Uzun L, Besirli N, Denizli A (2004) Poly(ethylene glycol dimethacrylate-*N*-vinyl imidazole) beads for heavy metal removal. *J Hazard Mater* 106 B:93–99
- Bulut Y, Akçay G, Elma D, Serhatli IE (2009) Synthesis of clay-based superabsorbent composite and its sorption capability. *J Hazard Mater* 171:717–723
- Minisci F, Porto O (1974) Advances in homolytic substitution of heteroaromatic compounds. In: Katritzky AR, Boulton AJ (eds.) *Advances in heterocyclic chemistry*, vol 16. Academic Press, Inc, New York, pp 123–180
- Minisci F (1976) Recent aspects of homolytic aromatic substitutions. *Top Curr Chem* 62:1–48
- Minisci F, Citterio A (1980) Polar effects in *free-radical* reactions in synthetic *chemistry*. In: Williams GH (ed.) *Advances in free radical chemistry*, vol 6. Heyden & Sons Ltd, London, 65–153
- Antonjetti M, Conrad J (1994) Synthesis of very highly ordered liquid crystalline phases by complex formation of polyacrylic acid with cationic surfactants. *Angew Chem Intern Ed* 33:1869–1870
- Antaya H, Richard-Lacroix M, Pellerin C (2010) Electrospinning as a new method for preparing pure polymer complexes. *Macromolecules* 43:4986–4990
- Neira A, Tarraga M, Catalan R (2007) Degradation of polyacrylic acid by Fenton’s reagent. *J Chil Chem Soc* 52:1314–1317
- Tekin N, Dinçer A, Demirbaş Ö, Alkan M (2006) Adsorption of cationic polyacrylamide onto sepiolite. *J Hazard Mater* B134:211–219
- Zhao G, Zhang H, Fan Q, Ren X, Li J, Chen Y, Wang X (2010) Sorption of copper (II) onto super-adsorbent of bentonite-polyacrylamide composites. *J Hazard Mater* 173:661–668
- Yetimoğlu EK, Kahraman MV, Ercan OE, Akdemir ZS, Apohan NK (2007) *N*-vinylpyrrolidone/acrylic acid/2-acrylamido-2-methylpropane sulfonic acid based hydrogels: synthesis, characterization and their application in the removal of heavy metals. *React Funct Polym* 67:451–460
- Zheng Y, Hua S, Wang A (2010) Adsorption behavior of Cu²⁺ from aqueous solutions onto starch-g-poly(acrylic acid)/sodium humate hydrogels. *Desalination* 263:170–175
- Bunting JW, Thong KM (1970) Stability constants for 1:1 metal-carboxylate complexes. *Can J Chem* 48:1654–1656
- Kostić I, Anđelković T, Nilković R, Bojić A, Purenović M, Blagojević Anđelković D (2011) Copper(II) and lead(II) complexation by humic acid and humic S-like ligands. *J Serb Chem Soc* 76:1325–1336
- Deleuze H, Schultze X, Sherrington DC (2000) Synthesis of porous supports containing *N*-(*p*-hydroxyphenyl)- or *N*-(3-(4-dihydroxybenzyl) maleimide-anchored titanates and application as

- catalysts for transesterification and epoxidation reactions. *J Polym Sci Part A Polym Chem* 38:2879–2886
- 36 Yılmaz SV, Kul D, Erdöl M, Özdemir M, Abbasoğlu R (2007) Synthesis of a novel crosslinked superabsorbent copolymer with diazacyclooctadecane crown ether and its sorption capability. *Eur Polym J* 43:1923–1932
- 37 Lagergren S (1898) Zur theorie der sogenannten adsorption gelöster stoffe, *K Sven Vetenskapsakad. Handl* 24:1–39
- 38 Ho YS, McKay G (1999) Pseudo-second order model for sorption processes. *Proc Biochem* 34:451–465
- 39 Freundlich HMF (1906) Über die *adsorption* in losungen. *Z Phys Chem (Leipzig)* 57:385–470
- 40 Langmuir I (1916) The constitution and fundamental properties of solids and liquids Part I. Solids. *J Am Chem Soc* 38:2221–2295
- 41 Temkin MI, Pyzhev V (1940) Kinetics of ammonia synthesis on promoted iron catalyst. *Acta Phys Chim USSR* 12:327–356
- 42 Zhao X, Zhang G, Jia Q, Zhao C, Zhou W, Li W (2011) Adsorption of Cu(II), Pb(II), Co(II), Ni(II), and Cd(II) from aqueous solution by poly(aryl ether ketone) containing carboxyl groups (PEK-L): equilibrium, kinetics, and thermodynamics. *Chem Eng J* 171:152–158

